UDC 546:547 EDN: RVNUAO

STUDY THE EFFICIENCY OF TITANIUM DIOXIDE NANOPARTICLES FOR WATER TREATMENT FROM CONGE RED DYE

D.A. Yass duaaayad@mtu.edu.iq
A.M. Abbas ahmed.m.a.@ihcoedu.uobaghdad.edu.iq

University of Baghdad, Baghdad, Iraq

Abstract

A modified chemical method was used to prepare titanium dioxide nanoparticles (TiO_2 NPs), which were diagnosed by several techniques: X-ray diffraction, Fourier transform infrared, field emission scaning electron microscopy, energy disperse X-ray, and UV-visible spectroscopy, which proved the success of the preparation process at the nanoscale level. Where the titanium oxide particles have an average particle size equal to 6.8 nm, titanium dioxide particles were used in the process of adsorption of Congo red dye from its aqueous solutions using a batch system. The titanium oxide particles gave an adsorption efficiency of Congo red dye up to more than 79 %. The experimental data of the adsorption process were analyzed with kinetic models and it was found that the process follows false second order, which suggests that the adsorption of Congo red dye is of the chemical type. As a result of the foregoing, titanium oxide particles can be considered an efficient adsorbent surface in the field of organic pollutants and dyes in particular

Keywords

Nanoparticles, titanium dioxide, adsorption, Congo red dye, kinetic

Received 01.03.2024
Accepted 06.05.2024

Introduction. Water is used extensively in various sectors, including domestic, agricultural, and industrial. As a result, it is exposed to many pollutants, which leads to an increase in the toxicity of the aquatic environment [1]. As a result, a great danger is generated that increases with the increase in the percentage of polluted water in the environment. Cosmetics range and other shapes, textiles, dyeing, paper, tanning, cosmetics, etc. are used. Production of $7 \cdot 10^5$ tons of dyes per year, release of about 10 % from the environment by the textile sector and textile sector [2–4]. Pigments are attractive materials because of their beautiful appearance. But at the same time, they are considered carcinogenic substances and substances that block light from bodies of water, so their

presence in them constantly threatens human life [5]. For the purpose of controlling water pollution with dyes, these dyes must be removed before the polluted water is released into the aquatic environment. Among these dyes is Congo red (CR), which is an anionic dye, which will be targeted in this study because the presence of dyes in the water shows undesirable properties that are harmful to the lives of all living organisms [6]. The Congo red dye solution has the potential to become benzidine, which is a significant risk to human health due to its ability to cause skin and eye damage and illness. There are several chemical, physical, and biological methods to remove (CR) dye, but most of them are expensive and complex, and some of them are inefficient [7, 8]. One of these methods is adsorption, which is characterized by being easy and simple to implement when dealing with liquid waste, its low costs, its efficiency, and the abundance of surfaces used in its application [9–12]. Nanomaterials are advanced materials at the nano level because they connect macromaterials and molecular materials. Materials that have at least one dimension ranging from 1 to 100 nanometers and have different shapes. Their shapes and sizes allow them to have a large surface area, resulting in high effectiveness. Nanoparticles (NPs) are employed in daily life and can be utilized in a range of healthcare, chemical, and water treatment applications [14, 15].

Titanium dioxide (TiO_2) exists in many forms, including rutile, which is uniformly crystalline and stable and is formed at a high temperature of up to 800 °C. While in the amorphous form, another form is called anatase, which is a random irregular form that forms at an average temperature of 350 °C. TiO_2 NPs have distinctive properties in terms of stability, are cheap, and are considered strong oxidizing materials, which makes them applicable in several fields. However, there are limitations that limit the use of titania due to the recombination of the electron gap as well as the small surface area [16, 17].

Therefore, several studies included the use of nanomaterials, including tin oxide nanoparticles, which were prepared by the sol-gel method, was characterized using several techniques (TGA, GC-MASS, XRD, and SEM). It was used to remove (CR) dye from aqueous media, where batch experiments were conducted to study adsorption. The results showed that SnO_2 catalysts had a high efficiency (84.41 %) after 60 min of exposure time, and this reflects the importance of the results for designing effective adsorbing materials [18].

Another study included the use of *Sansevieria* leaf extract for the synthesis of titanium dioxide NPs. Which was used in tests of the association of the azo dye CR with nanoparticles through adsorption from its aqueous solution. The experimental data were analyzed kinematically and proven to follow pseu-

do-second order. It also analyzed thermodynamics and proved that the adsorption process on the TiO_2 (NPs) surface is a physical, spontaneous, and endothermic process [19]. This investigation is intended to synthesize nano-sized titanium dioxide TiO_2 by modifying chemical methods, compositions, particle morphology, and efficacy performance.

Material and methods. The chemicals required were titanyl sulfate ($TiOSO_4$, *Sigma-Aladrich*) and hydrogen peroxide (H_2O_2, *Merck*) for the preparation of TiO_2 NPs by a modified chemical method for CR ($C_{32}H_{22}N_6Na_2O_6S_2$, *Merck*) adsorption efficiency (Fig. 1), and distilled water was used as a solvent.

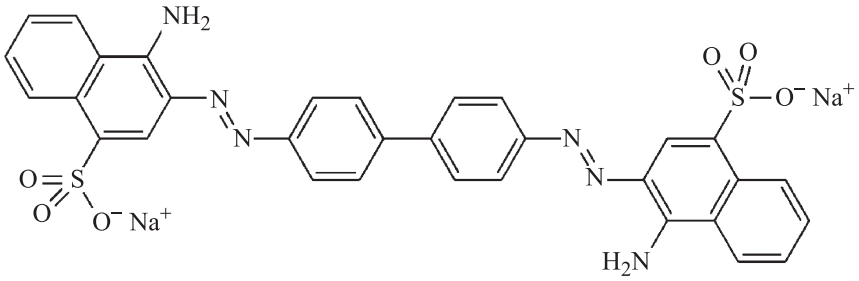

Fig. 1. Structure of CR

Preparation of nanoparticles of titanium. It was prepared by placing 2 gm of titanyl sulfate in a 300 ml beaker containing 20 ml of distilled water and exposing it to ultrasonic waves (Ultrasonic (ISO LAB), *Laborgerate GmbH*) 15 min, and then gradually adding 50 ml of cooled hydrogen peroxide (50 %) at a temperature of 10 °C. After preparing the reaction mixture and exposing it to ultrasound for 45 min, it was observed that effervescence occurred because it is an exothermic reaction with the formation of a precipitate, which represents titanium nanoparticles, where it is left for (24 h), filtered, washed, and dried at a temperature of 40 °C (*Daihan Labtech Oven, LDO-60e*, South Korea) for 1 h, and then burned. The precipitate is kept at a temperature of 400 °C (*Furnaces oven Vindon LTD, OLDHAM,* England) for 1 h and kept in a tightly closed container away from moisture. Then it is diagnosed using several techniques (FT-IR *Shimadzu*, Japan, XRD, Siemens model *D500*, Germany, EDX Oxford instruments, UK, and FE-SEM *ZEISS* model *Sigma VP-UK*).

Adsorption experiments. The adsorption experiment was conducted by applying a continuous system by taking a weight (0.01 g) of the prepared titanium dioxide TiO_2 and bringing it into contact with the volume (100 ml) of CR dye solution at a concentration of 50 mg/L by using a water bath shaker (*Labtech*, South Korea) at laboratory temperature, 150 rpm agitation speed,

and over time periods (0–120 min), and each sample is separated by a centrifuge in order to be measured. Each solution is used by the spectrometer (*Shimadzu 1800*, Japan), and the amount of adsorbed dye and the percentage of adsorption (A, %) are calculated through the following equations (1), (2), respectively [20]:

$$A = \frac{C_0 - C_t}{C_0} \cdot 100\,\%, \quad q_e = \frac{C_0 - C_t}{m} V,$$

where C_0, C_t are the CR dye concentrations at time ($t = 0$, t) respectively; V (L) represents the volume of CR aqueous solution, whereas m (g) symbolizes the TiO_2 adsorbent dose.

Results and discussion. *X-ray diffraction analysis.* The X-ray diffraction (XRD) diffractogram of TiO_2 NPs is presented in Fig. 2. The percentage of anatase was found to be high compared to other forms of titania and the reference sample (99.7 % of anatase, *Aldrich*). This is due to the heat treatment to which titanium oxide was subjected during the preparation process, which is 400 °C, which produces a high percentage of the anatase form of titania. Figure 2 by matching with JCPDS (Joint Committee on Powder Diffraction Standards) card No. 78-2486, the characteristic peaks in the 2θ range of 10° < 2θ < 80° at 25.64, 38.09, 48.20, 54.82, and 63°, where found to match 6° with values of Miller indices (hkl): (1 0 1), (0 0 4), (2 0 0), (1 0 5), and (2 0 4), respectively, which indicates that the dominant form is the anatase form of titania [21].

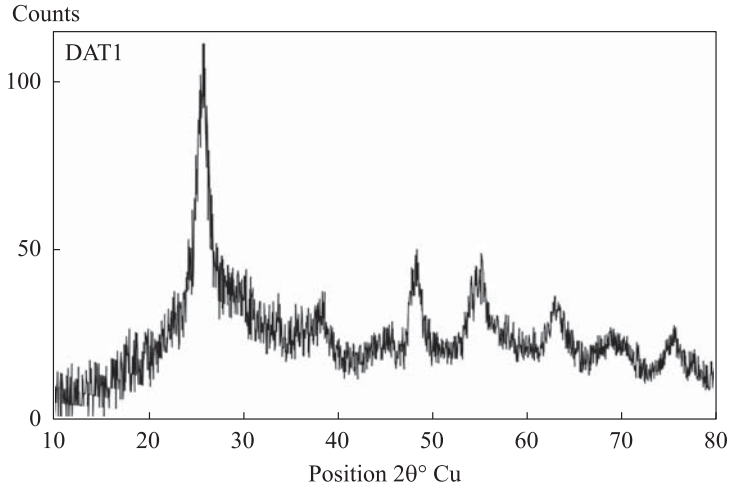

Fig. 2. XRD of TiO_2 NPs

We used the Debye — Scherer equation to obtain the crystallite size [22]: $S_{hkl} = k\lambda / (b \cos\theta)$, where S_{hkl} is the average crystallite size (nm); k is the Scherer constant (0.89); λ is the incident X-ray wavelength; b is the FWHM (full

width high maximum); θ is the Bragg diffraction angle. The average crystallite size is 6.8 nm.

Fourier transform infrared analysis (FT-IR). Figure 3 shows the Fourier transform infrared (FT-IR) spectra of TiO_2 NPs, clearly showing tree bands within a range between 400 and 4000 cm^{-1}. The first broadest band was observed at 3194 cm^{-1}, corresponding to the hydroxyl group O–H (stretching vibration) of the TiO_2 NPs which it is noted that there is a broad peak, which may be due to the titanium dioxide nanoparticles having hydroxyl groups on the surface, which reflects the symmetrical and asymmetrical stretching vibrations of it, or the low percentage of crystallinity reflects the broad peak, or the presence of hydroxyl groups leads to the broadening of the peak because it is associated with the presence of a percentage of moisture in the sample. The second small sharp band is observed around 1635 cm^{-1}, corresponding to water and Ti–OH (bending modes); the third group peaks are observed between 400 and 1000 cm^{-1} and the links stretch titanium–oxygen (Ti–O) (stretch) [23, 24].

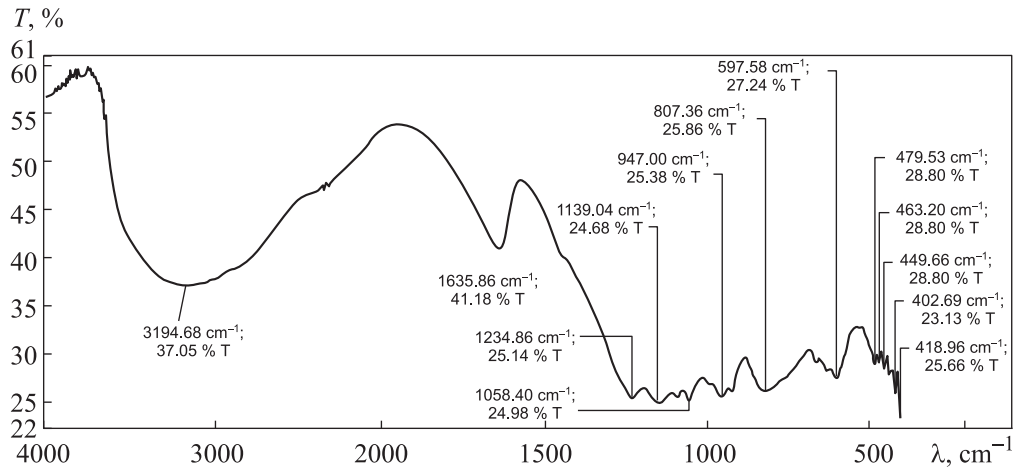

Fig. 3. FT-IR of TiO_2 NPs

Field emission scanning electron microscope (FE-SEM). Figure 4 shows an image of titanium oxide NPs at the level of 200 nm, where the image shows clusters of spherical titania particles, which have an average size of 35 nm. The size of titanium dioxide NPs from field emission scanning electron microscope (FE-SEM) measurment is larger than the XRD measurements, because the measurement is of aggregates of titanium dioxide nanoparticles, which gives larger sizes compared to measuring the size of titanium dioxide NPs from XRD measurement.

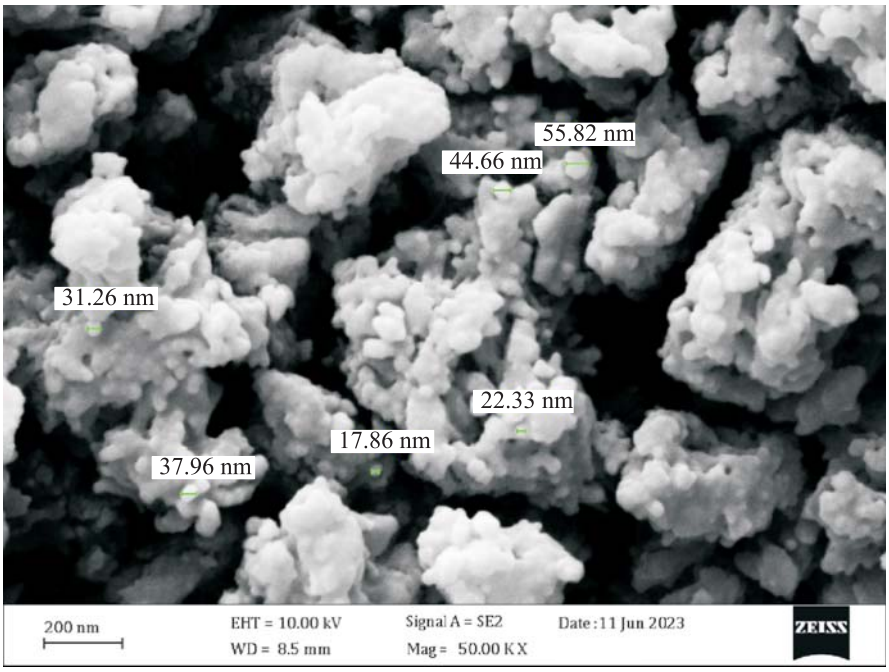

Fig. 4. FE-SEM image of TiO_2 NPs

Energy disperse X-Ray analysis. Energy disperse X-Ray (EDX) analysis of TiO_2 NPs was performed to determine the composition of the prepared TiO_2 NPs, as shown in Fig. 5, where it was found that the highest weight percentage was for Ti at 76.9 %, oxygen (O) at 19 %, and another difference was observed for carbon (C) at 4 %. It indicates the presence of impurities as a result of the process of intense heating of titanium oxide particles, and according to the previous results, this indicates the formation of titanium dioxide nanoparticles in a large proportion, as shown in Fig. 5.

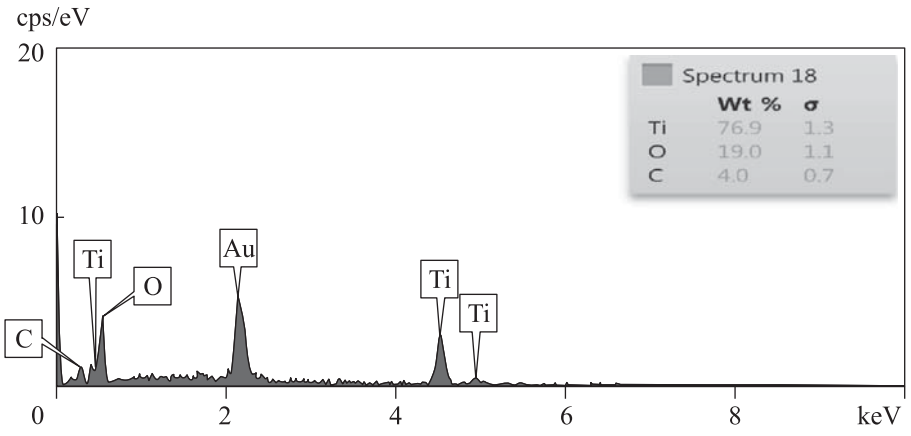

Fig. 5. EDX spectrum of TiO_2 NPs

Study of Congo red dye adsorption. The effect of the CR dye adsorption duration from 15 to 180 min was determined while maintaining other parameters such as pH 7, starting CR concentration of 40 mg/L, TiO_2 NPs weight of 0.01 g, and 150 rpm shaking speed at 298 K. The effects of agitation time on the adsorption of CR dye are shown in Fig. 6, *a*. The quantity of CR dye adsorbed increases with passing time and reaches equilibrium in around 150 min, after which the rate of removal remains constant. This might be a reference to the possibility of CR molecules adhering to a wide surface area on TiO_2 adsorbent for at least 150 min after the unoccupied surface sites have been saturated, with adsorption efficiency up to 88 %, as shown in Fig. 6, *b*. While we notice from

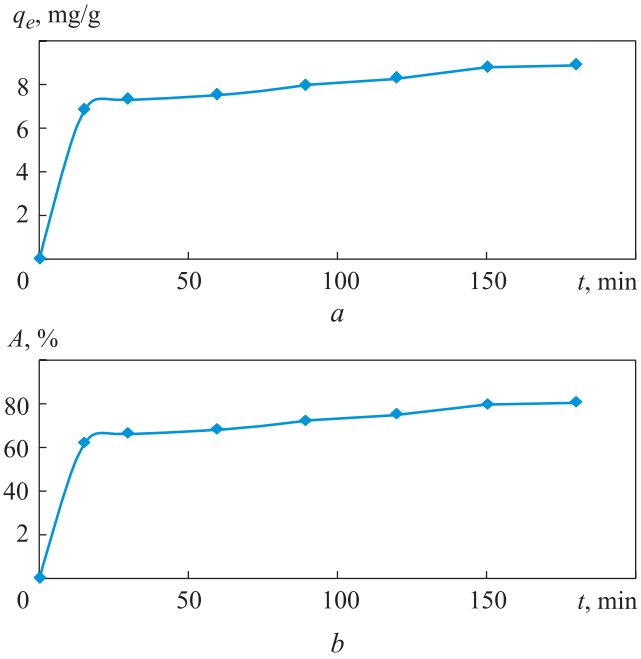

Fig. 6. Effect of contacting time on the quantity (*a*) and percent (*b*) adsorption of CR dye on TiO_2 NPs

Fig. 7 that the electronic spectra of CR dye beginning and during of adsorption decreases in intensity with the passage of time and with no displacement, which indicates the occurrence of CR dye adsorption onto TiO_2 NPs [25].

Kinetics of adsorption. The experimental data were analyzed by kinetic models. The linearized pseudo-first-order (PFO) and pseudo-second-order (PSO) models have been applied [26]:

$$\ln(q_e - q_t) = \ln q_e - k_1 t, \quad \frac{1}{q_t} = \frac{1}{k_2 q_e^2} + \frac{t}{q_e},$$

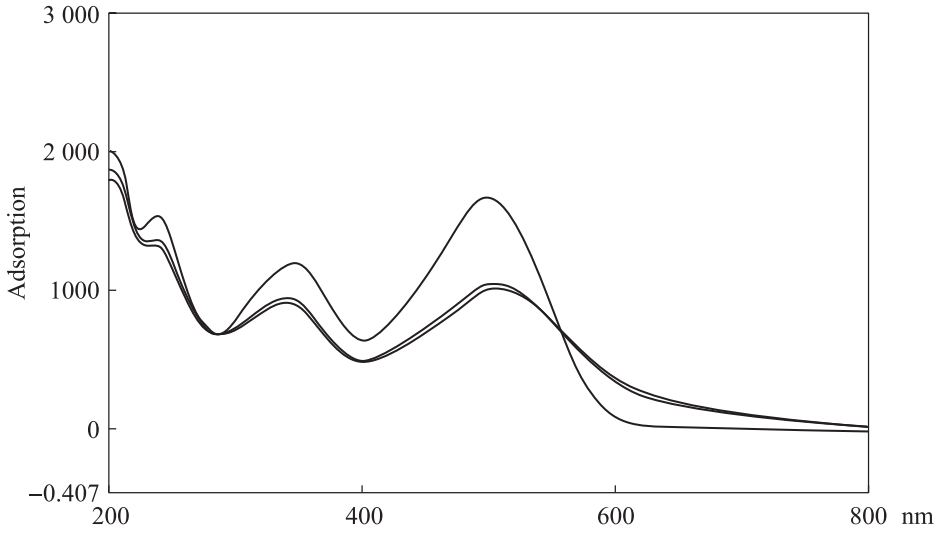

Fig. 7. UV-Vis spectra of CR dye beginning and during the adsorption at different times

where q_t, q_e are the amounts of CR dye molecules adsorbed on the TiO_2 NPs at time t and at equilibrium (mg/g); k_1 (min^{-1}), k_2 ($g \cdot mg^{-1} \cdot min^{-1}$) are the rate constants of PFO and PSO, respectively. The linear plots of $\ln(q_e - q_t)$ versus (t) and t/q_t versus t are employed to calculate k_1, q_e values for PFO, and k_2, q_e values for PSO, as shown in Fig. 8. Table lists the PFO and PSO constants for

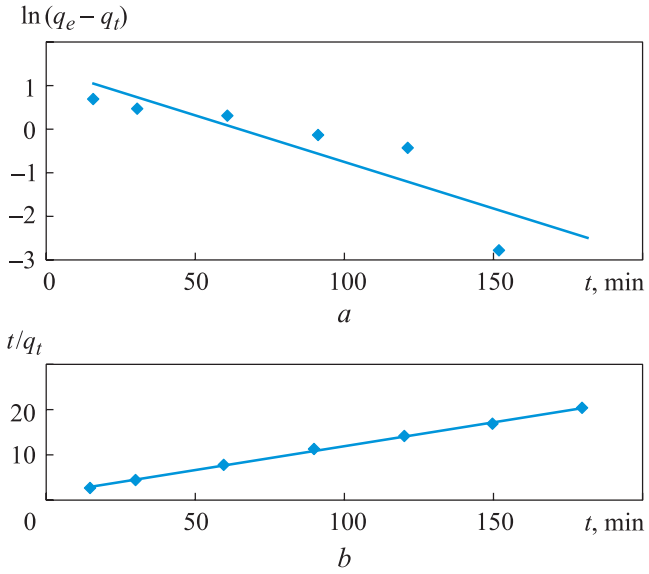

Fig. 8. PFO plot of kinetics (*a*) and PSO plot for the adsorption (*b*) of CR dye on TiO_2 NPs:

a) $y = -0.0216x + 1.3721$, $R^2 = 0.7685$; *b*) $y = 0.1079x + 1.0471$, $R^2 = 0.9959$

the adsorption process. As shown in Table, the values of correlation coefficient R^2 for PSO were higher than those for PFO. Also, the values of q_e experimental ($q_{e.\,\mathrm{exp}}$) and q_e calculated ($q_{e.\,\mathrm{cal}}$) were matched well using PSO kinetic models, suggesting that the mechanisms of adsorption are related to both adsorbent and adsorbate [27, 28].

PFO and PSO kinetics data for adsorption of CR dye on TiO_2 NPs (298 K)

Surface	PFO			
	k_1, min^{-1}	$q_{e.\,\mathrm{cal}}$, mg/g	$q_{e.\,\mathrm{exp}}$, mg/g	R^2
TiO_2 NPs	0.022	3.944	8.939	0.769
	PSO			
	k_2, $\mathrm{g \cdot mg^{-1} \cdot min^{-1}}$	$q_{e.\,\mathrm{cal}}$, mg/g	$q_{e.\,\mathrm{exp}}$, mg/g	R^2
	0.011	9.268	8.939	0.996

Conclusion. Through the current work and the diagnostic techniques used (XRD, FT-IR, EDX and FE-SEM), we conclude the success of the modified chemical method in preparing titanium oxide nanoparticles with a nanosize rate of 6.8 nm. It has an adsorption efficiency of more than 79 % for removing CR dye from its aqueous solution. Depending on the kinetic data, we found that the CR dye adsorption process has a chemical nature.

REFERENCES

[1] Manisha V., Haritash A.K. Photocatalytic degradation of amoxicillin in pharmaceutical wastewater: a potential tool to manage residual antibiotics. *Environ. Technol. Innov.*, 2020, vol. 20, art. 101072. DOI: https://doi.org/10.1016/j.eti.2020.101072

[2] Fawzy M.A., Gomaa M. Use of algal biorefinery waste and waste office paper in the development of xerogels: a low cost and eco-friendly biosorbent for the effective removal of Congo red and Fe(II) from aqueous solutions. *J. Environ. Manage*, 2020, vol. 262, art. 110380. DOI: https://doi.org/10.1016/j.jenvman.2020.110380

[3] Yagub M.T., Sen T.K., Afroze S., et al. Dye and its removal from aqueous solution by adsorption: a review. *Adv. Colloid Interface Sci.*, 2014, vol. 209, pp. 172–184. DOI: https://doi.org/10.1016/j.cis.2014.04.002

[4] Parvin S., Biswas B.K., Rahman A. Study on adsorption of Congo red onto chemically modified egg shell membrane. *Chemosphere*, 2019, vol. 236, art 124326. DOI: https://doi.org/10.1016/j.chemosphere.2019.07.057

[5] Pathania D., Sharma A., Siddiqi Z. Removal of Congo red dye from aqueous system using *Phoenix dactylifera* seeds. *J. Mol. Liq.*, 2016, vol. 219, pp. 359–367. DOI: https://doi.org/10.1016/j.molliq.2016.03.020

[6] Adebayo M.A., Jabar J.M., Amoko J.S., et al. Coconut husk-raw clay-Fe composite: preparation, characteristics and mechanisms of Congo red adsorption. *Sci. Rep*., 2022, vol. 12, no. 1, pp. 1–12. DOI: https://doi.org/10.1038/s41598-022-18763-y

[7] Alamrani N.A., AL-Aoh H.A. Elimination of Congo red dye from industrial wastewater using *Teucrium polium L.* as a low-cost local adsorbent. *Adsorpt. Sci. Technol*., 2021, vol. 2021. DOI: https://doi.org/10.1155/2021/5728696

[8] Mishra S., Cheng L., Maiti A. The utilization of agro-biomass/byproducts for effective bio-removal of dyes from dyeing wastewater: a comprehensive review. *J. Environ. Chem. Eng*., 2021, vol. 9, iss. 1, art. 104901. DOI: https://doi.org/10.1016/j.jece.2020.104901

[9] Wekoye J.N., Wanyonyi W.C., Wangila P.T., et al. Kinetic and equilibrium studies of Congo red dye adsorption on cabbage waste powder. *Environ. Chem. Ecotoxicol*., 2020, vol. 2, pp. 24–31. DOI: https://doi.org/10.1016/j.enceco.2020.01.004

[10] Jasim M.A., Abbas A.M. Equilibrium and thermodynamic study of malachite green & phenol red dyes adsorption from aqueous solution by use algae biomass. *Journal of Global Pharma Technology*, 2019, vol. 11, no. 2, pp. 21–31.

[11] Dhafir T.A., Dawood A.H., Khalaf Q.Z., et al. Removal of methyl orange from aqueous solution by Iraqi bentonite adsorbent. *Ibn Al-Haitham J. Pure Appl. Sci*., 2012, vol. 25, no. 2, pp. 328–339.

[12] Abbas A.M., Mohammed Y.I., Himdan T.A. Adsorption of anionic dye from eqeous solution by modified synthetic zeolite. *Ibn Al-Haitham J. Pure Appl. Sci.*, 2015, vol. 28, no. 2, pp. 52–68.

[13] Ghulam N., Qurat-ul-Aain N.R., Khalid M., et al. A review on novel eco-friendly green approach to synthesis TiO_2 nanoparticles using different extracts. *J. Inorg. Organomet. Polym. Mater*., 2018, vol. 28, no. 4, pp. 1552–1564.
DOI: https://doi.org/10.1007/s10904-018-0812-0

[14] Abd S.S., Abbas A.M. Preparation, characterization and adsorption capacity of bauxite-carbon nanotube composite. *Nat. Environ. Pollut. Technol.*, 2019, vol. 18, no. 3, pp. 863–869.

[15] Alaa A.M., Hadi S.A., Ali A.A. Kinetic, isotherm, and thermodynamic study of Bismarck brown dye adsorption onto graphene oxide and graphene oxide-grafted-poly (n-butyl methacrylate-co-methacrylic acid). *Baghdad Sci. J.*, 2022, vol. 19, no. 1, pp. 132–140.

[16] Ghulam N., Waseem R., Tahir M.B. Green synthesis of TiO_2 nanoparticle using cinnamon powder extract and the study of optical properties. *J. Inorg. Organomet. Polym. Mater*., 2020, vol. 30, no. 4, pp. 1425–1429.
DOI: https://doi.org/10.1007/s10904-019-01248-3

[17] Al-Kazragi M.A.R., Al-Heetimi D.T.A. Removal of toxic dye (Rhodamine B) from aqueous solutions by natural smectite (SMC) and SMC-nanoTiO_2. *Desalination Water Treat.*, 2021, vol. 230, pp. 276–287.

[18] Elaziouti A., Laouedj N., Vannier R. Adsorption of Congo red azo dye on nanosized SnO_2 derived from sol-gel method. *Int. J. Ind. Chem.*, 2016, vol. 7, no. 1, pp. 53–70. DOI: https://doi.org/10.1007/s40090-015-0061-9

[19] Rasha T.S., Dunya E.A. Adsorption of azo dye onto TiO_2 nanoparticles prepared by a novel green method: isotherm and thermodynamic study. *Iraqi J. Sci.*, 2023, vol. 64, no. 8, pp. 4679–4692. DOI: https://doi.org/10.24996/ijs.2023.64.8.5

[20] Jasim M.A., Abbas A.M., Radhi I.M. Preparation and characterization of biomass-alumina composite as adsorbent for safranine-o dye from aqueous solution at different temperatures. *AIP Conf. Proc.*, 2021, vol. 2372, iss. 1, art. 120001.
DOI: https://doi.org/10.1063/5.0068746

[21] Chen J., Zhang Li. NH_4Cl-assisted low temperature synthesis of anatase TiO_2 nanostructures from Ti powder. *Mater. Lett.*, 2009, vol. 63, iss. 21, pp. 1797–1799.
DOI: https://doi.org/10.1016/j.matlet.2009.05.042

[22] Zhang J., Zhou P., Liu J., et al. New understanding of the difference of photocatalytic activity among anatase, rutile and brookite TiO_2. *Phys. Chem. Chem. Phys.*, 2014, vol. 16, iss. 38, pp. 20382–20386. DOI: https://doi.org/10.1039/C4CP02201G

[23] Nadica D., Abazovic M., Comor M., et al. Photoluminescence of anatase and rutile TiO_2 particles. *J. Phys. Chem. B*, 2006, vol. 110, iss. 50, pp. 25366–25370.
DOI: https://doi.org/10.1021/jp064454f

[24] Mugundan S., Rajamannan G., Viruthagiri N., et al. Synthesis and characterization of undoped and cobalt-doped TiO_2 nanoparticles via sol-gel technique. *Appl. Nanosci.*, 2015, vol. 5, no. 4, pp. 449–456. DOI: https://doi.org/10.1007/s13204-014-0337-y

[25] Ahmed M.A., Yousif I.M., Taki A.H. Adsorption kinetic and thermodynamic study of congo red dye on synthetic zeolite and modified synthetic zeolite. *Ibn Al-Haitham J. Pure Appl. Sci.*, 2015, vol. 28, no.1, pp. 54–72.

[26] Benjelloun M., Miyah Y., Evrendilek G.A., et al. Recent advances in adsorption kinetic models: their application to dye types. *Arab. J. Chem.*, 2021, vol. 14, iss. 4, art. 103031. DOI: https://doi.org/10.1016/j.arabjc.2021.103031

[27] Bentahar S., Dbik A., El Khomri M., et al. Study of removal of Congo red by local natural clay. *St. Cerc. St. CICBIA*, 2016, vol. 17, no. 3, pp. 295–305.

[28] Faraj R.A.S., Abbas A.M. Loading and activating a carbon surface and applied for Congo red adsorption, kinetic study. *J. Phys.: Conf. Ser.*, 2021, vol. 1879, art. 022076. DOI: https://doi.org/10.1088/1742-6596/1879/2/022076

Yass D.A. — Ph.D. Student, Department of Chemistry, College of Education for Pure Sciences (Ibn al-Haytham), University of Baghdad (Baghdad, Karrada, Al-Jadriya, Iraq).

Abbas A.M. — Professor, Department of Chemistry, College of Education for Pure Sciences (Ibn al-Haytham), University of Baghdad (Baghdad, Karrada, Al-Jadriya, Iraq).

Please cite this article as:

Yass D.A., Abbas A.M. Study the efficiency of titanium dioxide nanoparticles for water treatment from Conge red dye. *Herald of the Bauman Moscow State Technical University, Series Natural Sciences*, 2024, no. 4 (115), pp. 121–131. EDN: RVNUAO